Very precise orbits of 1998 Leonid meteors

HANS BETLEM[1], PETER JENNISKENS[2]*, JAAP VAN 'T LEVEN[1], CASPER TER KUILE[1], CARL JOHANNINK[1],
HAIBIN ZHAO[3], CHENMING LEI[3], GUANYOU LI[3], JIN ZHU[4], STEVE EVANS[5] AND PAVEL SPURNÝ[6]

[1]Dutch Meteor Society, Lederkarper 4, 2318 NB Leiden, The Netherlands
[2]SETI Institute, NASA Ames Research Center, Mail Stop 239-4, Moffett Field, California 94035, USA
[3]Purple Mountain Observatory, 2 West Beijing Road, 210008 Nanjing, Peoples Republic of China
[4]Beijing Astronomical Observatory, Chinese Academy of Sciences, Beijing, Peoples Republic of China
[5]BAA Meteor Section, 1 Hall Cottages, Little Thurlow, Haverhill, Suffolk, CB9 7HY, United Kingdom
[6]Astronomical Institute, Ondrejov Observatory, 251 65 Ondrejov, Czech Republic
*Correspondence author's e-mail address: peter@max.arc.nasa.gov

Abstract–Seventy-five orbits of Leonid meteors obtained during the 1998 outburst are presented. Thirty-eight are precise enough to recognize significant dispersion in orbital elements. Results from the nights of 1998 November 16/17 and 17/18 differ, in agreement with the dominant presence of different dust components. The shower rate profile of 1998 November 16/17 was dominated by a broad component, rich in bright meteors. The radiant distribution is compact. The semimajor axis is confined to values close to that of the parent comet, whereas the distribution of inclination has a central condensation in a narrow range. On the other hand, 1998 November 17/18 was dominated by dust responsible for a more narrow secondary peak in the flux curve. The declination of the radiant and the inclination of the orbit are more widely dispersed. The argument of perihelion, inclination, and the perihelion distance are displaced. These data substantiate the hypothesis that trapping in orbital resonances is important for the dynamical evolution of the broad component.

INTRODUCTION

The real possibility of a Leonid meteor storm in 1998 November was a strong motivation for continuing our ongoing effort to monitor the activity of the shower by visual, photographic, and video techniques (Jenniskens, 1996; Betlem *et al.*, 1997; Langbroek, 1999). The effort was started in 1994, when the Leonid shower first showed enhanced activity in association with the 1998 return of parent comet 55P/Tempel–Tuttle (Jenniskens, 1996). Each subsequent observing campaign sampled debris at a unique position behind the parent comet and at a unique moment in time (Jenniskens and Betlem, 2000).

The 1998 campaign provided support for NASA's Leonid multi-instrument aircraft campaign (Leonid MAC). Ground stations were set up in the Peoples Republic of China at locations +1 and +2 time zones west from Leonid MAC at Okinawa, Japan (for a map, see Jenniskens and Butow, 1999). During a storm, it is possible to measure the orbits and debris distribution of relatively recent cometary ejecta at an unprecedented precision for addressing outstanding questions in meteor physics and meteoroid stream dynamics (Ceplecha *et al.*, 1998; Jenniskens, 1998). The purpose of the ground campaign was to measure the meteor flux and to measure precise meteor trajectories and orbits of relatively bright meteors. The large separation of the two sites enhanced chances that at least one site would have clear weather at the time of the storm. Here we report on the photographic results of this expedition.

METHOD

Of all potential observing sites that were suitably located for viewing the predicted peak, China offered the best prospects for good weather in the middle of November. In an effort coordinated by researchers at Purple Mountain Observatory in Nanjing, a cooperative agreement was set up between the Royal Dutch Academy of Sciences (KNAW) and the Chinese Academy of Sciences (CAS). This enabled 17 members of the Dutch Meteor Society to deploy some 1050 kg of equipment at two remote observing sites. The effort was strengthened by the participation of Chinese, U.S., and Czech (amateur) astronomers and covered six nights around the peak of the shower.

This "1998 Sino-Dutch Leonid Expedition" consisted of two double station networks for stereoscopic measurements. The first network was operated from the province of Hebei, where the main station was located at the Xing Long Observatory (40°24' N; 117°35' E), ~150 km northeast of Beijing. Local organization was in the hands of the Beijing Astronomical Observatory. At Xing Long, seven observers settled with platforms of small (35 mm format) cameras with 50 mm f1.8 optics and equipped with crystal controlled rotating shutters (Fig. 1). Fifteen-minute exposures were made on 400 ASA black and white film (Kodak T-Max, Ilford HP5). The camera timing was automated. To increase the accuracy of deceleration measurements, we used a relatively high rotating shutter speed, producing 50 breaks per second. Low-light television cameras were used to monitor the bright meteors for accurate timings. A second station of small cameras was established in the village of Lin Ting Kou, at a distance of 85 km to the south, a favourable direction for triangulation, because the Leonid meteors move predominantly from east to west during the night.

The second network was established in the Province of Qinghai. The main station was the Delingha radio observatory (37°23' N; 97°44' E). Local organization was in the hands of Purple Mountain Observatory. At this site, an improved array was operated, consisting of six small (35 mm format) cameras equipped with relatively long (85 mm) focal length optics. Rotating shutters of 100 breaks per second were used for the 85 mm cameras and 75 breaks per second for the 50 mm cameras. Double station images were obtained from a second site near the village of Ulan ~65 km
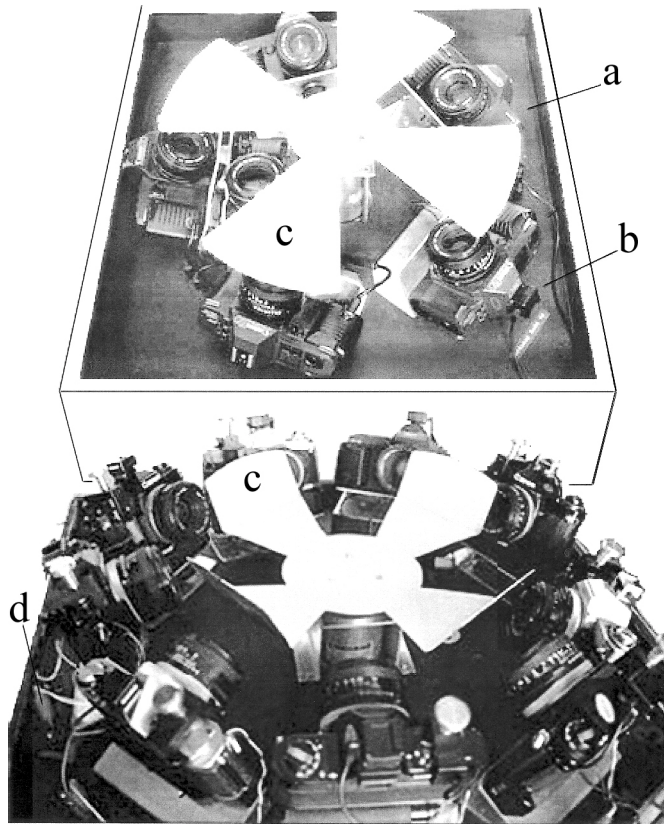
FIG. 1. Camera platforms of Xing-long station. A Canon T70 camera with command back (a) controls the opening and closing times of other cameras (b). The rotating shutter (c) provides speed information. Heating resistors (d) warm the cameras slightly above ambient temperature, in order to prevent condensation of moisture on the camera objectives.

FIG. 2. Example of a double-station meteor. (a) Bright $M_{max} = -13.2$ magnitude Leonid (DMS 98041) as seen from primary station Xing-Long on 1998 November 16 at 21:26:45 UT. (b) Same meteor as photographed from secondary station Lin Ting Kou.

south-southeast of the Delingha Observatory. This site operated fourteen 50 mm f1.8 and six 85 mm f1.8 cameras. Visual observations provided the meteor timing at these locations.

Each set of photographs was reduced in the normal manner (*e.g.*, Betlem *et al.*, 1997) in an interactive way by using Astrorecord measuring software (version 3.02), developed by Marc de Lignie of the Dutch Meteor Society. A typical positional accuracy is 0.003°. Some images were also measured at the Ondrejov Astrorecord X-Y measuring table, which demonstrated the claimed accuracy (Table 1)

TABLE 1. Comparison of measurements with the interactive Astrorecord software program (left) and the Ondrejov Observatory Astrorecord X–Y measuring table (right) for 11 bright Leonid meteors.*

Code	q	q	$1/a$	$1/a$
DMS 98002	0.9830 ± 0.0003	0.9834 ± 0.0001	0.096 ± 0.044	0.093 ± 0.035
98003	0.9830 ± 0.0004	0.9828 ± 0.0002	0.122 ± 0.040	0.154 ± 0.025
98008	0.9831 ± 0.0002	0.9833 ± 0.0002	0.133 ± 0.038	0.101 ± 0.030
98011	0.9819 ± 0.0001	0.9819 ± 0.0001	0.054 ± 0.015	0.053 ± 0.015
98012	0.9832 ± 0.0003	0.9831 ± 0.0002	0.079 ± 0.030	0.089 ± 0.030
98015	0.9830 ± 0.0001	0.9830 ± 0.0001	0.082 ± 0.020	0.084 ± 0.020
98020	0.9813 ± 0.0002	0.9814 ± 0.0002	0.221 ± 0.028	0.209 ± 0.028
98023	0.9839 ± 0.0002	0.9837 ± 0.0001	0.115 ± 0.011	0.106 ± 0.013
98041	0.9838 ± 0.0001	0.9839 ± 0.0001	0.042 ± 0.034	0.075 ± 0.028
98043	0.9832 ± 0.0002	0.9832 ± 0.0003	0.135 ± 0.033	0.119 ± 0.052
98044	0.9831 ± 0.0001	0.9835 ± 0.0002	0.104 ± 0.022	0.102 ± 0.041
Average	0.9830 ±0.0002	0.9830 ± 0.0002	0.107 ± 0.029	0.108 ± 0.028

*The latter include all-sky images of the meteors from Xing Long.

and enabled photometry. The trajectories and orbits were calculated with FIRBAL (version 7.0), developed by Zdenek Ceplecha, Pavel Spurný, and Jiri Borovická of Ondrejov Observatory.

RESULTS

Although a meteor storm did not occur in 1998, large numbers of bright Leonid meteors provided a bounty of data. The two-station networks were operated during the nights of November 16/17, 17/18, and 18/19. Between 100 and 140 meteors were captured on film on each station, of which all but a few were Leonid meteors. One hundred thirty-six meteors were photographed from two stations (Fig. 2). Seventy of these provided accurate orbits. The results are summarised in Tables 2–4.

In addition, we report here on multi-station results from a network of small cameras of the BAA Meteor Section in the U.K. Five Leonid meteors were captured on the night of 1998 November 16/17. These results were analyzed in the same way as all others.

All data are from two stations only. Errors in the trajectory and orbit calculations were estimated by rigorous analysis of the propagation of measurement

errors. For meteors that have known times of appearance, the uncertainty in the result is determined mainly by the observed lengths of the meteor trails on both images, the angular distances to the radiant, and the convergence angle. In 12 cases, the uncertainty is determined by an unknown time of the meteor, causing a large error in right ascension.

The convergence angle is the angle between the two planes that are defined by the apparent direction of the meteor trajectory and the observing station. In the following analysis and plots, we will discuss only the data with convergence angles $Q > 11°$. Best results were obtained from long trails (and high Q), which were numerous in our data sample. The high shutter speed further improved the speed measurements. As a result, we obtained 38 precise trajectories and orbits with uncertainties in radiant <0.1° and speed <1.0 km/s.

Trajectories and Radiants

The radiant position is considered first, because it can be measured most precisely. The radiant is most closely related to observations and can be studied (nearly) independent of the measured speed, a combination of which makes up the more physically relevant orbital elements.

The geocentric radiant (RA_{Geo}, DEC_{Geo}) is the direction of the heliocentric meteor velocity vector before it is affected by Earth's gravity and deceleration, but after the Earth's velocity is added in a vector sum. In order to compare results at different positions in the Earth's orbit, each radiant needs to be corrected for a changing Earth's velocity vector. We arbitrarily chose the Earth at solar longitude 235.0 (J2000) as the point of reference. The changing vector of Earth causes a daily radiant drift of ΔRA = +0.99 per degree solar longitude and ΔDEC = –0.36 per degree. After this correction, we searched for the rotation of the meteoroid heliocentric velocity vector with changing λ_o from a shift in the mean radiant.

The radiant dispersion of Leonid meteors photographed in years of normal annual activity is shown in Fig. 3 (top) and is compared to the radiant distribution in years of meteor outbursts (Fig. 3, bottom). Data before 1980 were taken from the IAU database, whereas recent data are from our own observing efforts (Betlem et al., 1998; Jenniskens and Betlem, 2000). Note that during meteor outbursts, the radiant dispersion is significantly less than in off-season years, and the mean radiant is shifted. Also, radiants in recent years differ from those during the 1965 return.

The accuracy is good enough to recognize the intrinsic dispersion in the compact radiants of the outburst component. This is illustrated in Fig. 4, which shows the radiant positions from the different nights of 1998 November with different symbols. Error bars of individual solutions are given. The radiants on 1998 November 16/17 are significantly different from those of 17/18. For each data set, the dispersion is larger than the measurement error and is equal to 0.095 ± 0.020° for the data from 1998 November 16/17 and 0.14 ± 0.04° for the data of 1998 November 17/18 (1σ). The larger dispersion on 1998 November 17/18 is mainly manifested in declination.

We do not find a strong mass-dependence in the radiant distribution. Right ascension and declination do not change significantly over 14 magnitudes of meteor brightness, corresponding to a factor of 600 in meteoroid mass.

Orbits

The previous pattern is manifested too in the distribution of perihelion distance (q), argument of perihelion (ω), and inclination (I). These orbital elements are calculated from each meteoroid's
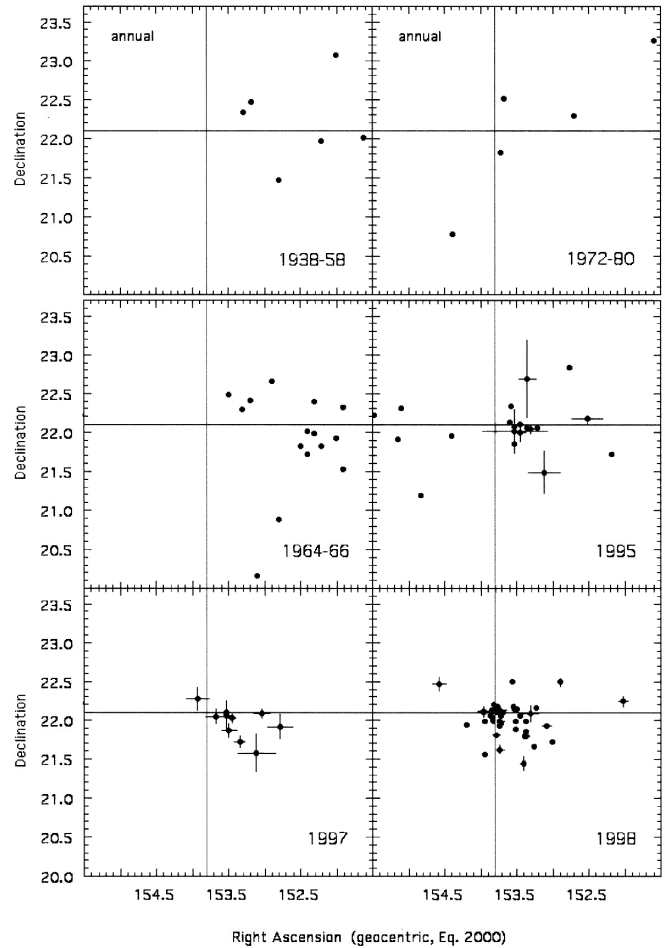
FIG. 3. Radiant dispersion of the Leonid shower from photographic records in different years. Top: off-season years. Bottom: years with significant outburst activity.
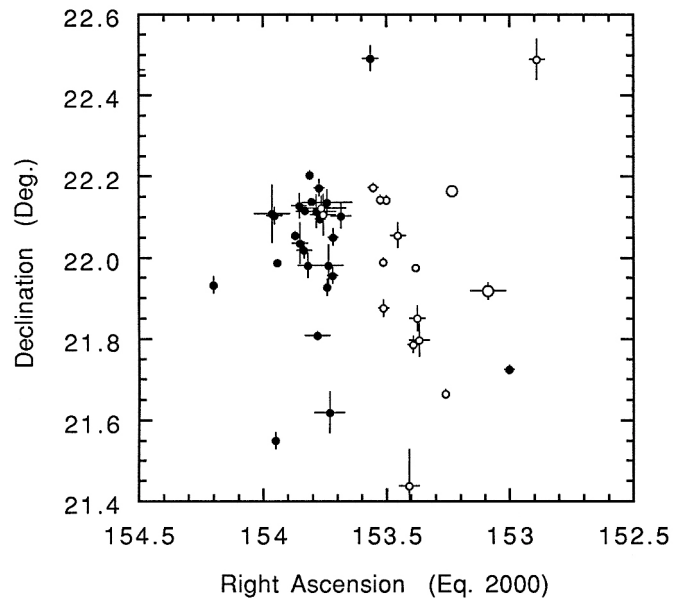
FIG. 4. Radiant dispersion during the 1998 return. Symbols discriminate between the nights of 1998 November 16/17 (•), 17/18 (○) and 18/19 (◯).

Betlem *et al.*

TABLE 2. Trajectory data of 1998 Leonid meteors.

	Code	mv	H_{beg}	H_{max}	H_{end}	RA_{Geo}	DEC_{Geo}	V_{inf}	V_g	V_h	COSZR	Q_{max}
DMS	98001	0	116.6	–	103.9	153.32 ± 0.28	22.23 ± 0.26	71.2 ± 0.9	70.0	40.8	0.20	46.2
	98002	–3	128.9	104.8	102.8	152.98 ± 0.03	22.33 ± 0.02	71.8 ± 0.0	70.6	41.4	0.22	31.0
	98003	–3	126.9	101.4	88.1	152.88 ± 0.06	21.93 ± 0.05	71.2 ± 0.0	70.0	40.7	0.25	18.7
	98004	–1	116.0	–	101.6	152.97 ± 0.04	22.29 ± 0.03	71.6 ± 0.1	70.4	41.2	0.27	38.1
	98008	–3	121.6	107.4	94.6	153.06 ± 0.01	22.35 ± 0.01	71.7 ± 0.3	70.5	41.3	0.43	30.0
	98011	–3	122.2	100.9	95.3	153.41 ± 0.01	22.22 ± 0.02	72.2 ± 0.2	71.0	41.8	0.49	30.1
	98101	–1	113.1	–	102.2	152.57 ± 1.13	22.43 ± 0.06	71.7 ± 0.5	70.5	41.2	0.29	16.4
	98012	–4	123.9	91.4	87.5	153.17 ± 0.03	22.39 ± 0.02	71.8 ± 0.3	70.6	41.4	0.53	24.8
	98102	–1	117.0	91.4	95.7	152.99 ± 0.02	22.38 ± 0.01	71.6 ± 0.3	70.4	41.2	0.32	26.0
	98013	–1	113.0	102.0	100.4	153.70 ± 0.17	22.25 ± 0.16	71.2 ± 0.2	70.1	40.9	0.55	37.0
	98103	0	117.2	–	102.8	153.08 ± 0.03	22.41 ± 0.03	71.6 ± 0.6	70.4	41.2	0.34	28.8
	98014	0	112.0	105.9	99.2	153.19 ± 0.07	22.39 ± 0.07	72.3 ± 1.7	71.1	41.9	0.58	36.8
	98015	–2	118.8	94.1	90.5	153.17 ± 0.00	22.27 ± 0.00	71.9 ± 0.2	70.7	41.5	0.58	33.9
	98105	–2	121.0	–	97.1	152.97 ± 0.06	22.26 ± 0.05	72.2 ± 0.2	71.0	41.8	0.39	20.2
	98106	–1	118.4	–	98.9	152.99 ± 0.10	22.41 ± 0.03	71.5 ± 0.2	70.3	41.1	0.45	16.2
	98107	0	117.6	–	101.1	153.22 ± 0.03	21.99 ± 0.07	71.5 ± 0.7	70.3	41.0	0.46	7.4
	98023	–14	124.8	84.4	73.2	153.08 ± 0.01	22.47 ± 0.01	71.6 ± 0.1	70.4	41.2	0.72	37.0
	98109	0	115.1	–	97.7	151.98 ± 1.97	22.29 ± 0.02	71.9 ± 0.6	70.7	41.4	0.54	18.4
	98027	0	109.6	–	91.6	152.98 ± 0.04	22.36 ± 0.03	71.6 ± 1.2	70.5	41.3	0.81	36.9
	98113	–2	116.7	–	94.3	153.09 ± 0.05	22.06 ± 0.01	71.7 ± 0.3	70.6	41.3	0.68	43.6
	98032	–1	118.3	97.1	93.1	151.34 ± 0.06	22.49 ± 0.06	71.1 ± 0.8	70.1	40.8	0.87	26.9
	98031	–1	117.1	99.7	91.5	153.90 ± 0.10	22.71 ± 0.09	71.4 ± 0.9	70.4	41.3	0.87	13.9
	98114	–1	115.0	–	96.9	153.27 ± 1.25	22.46 ± 0.06	71.6 ± 0.2	70.5	41.3	0.74	22.0
	98038	–2	121.0	90.7	88.4	153.05 ± 0.02	22.20 ± 0.02	71.5 ± 0.1	70.5	41.2	0.89	71.0
	98036	–2	117.9	92.5	70.2	153.14 ± 0.00	22.38 ± 0.00	71.5 ± 0.6	70.5	41.3	0.90	56.1
	98040	–1	115.0	101.8	97.2	153.17 ± 0.13	22.21 ± 0.13	71.3 ± 0.8	70.3	41.1	0.90	20.3
	98116	–4	121.7	–	88.7	153.06 ± 0.02	22.29 ± 0.02	71.6 ± 1.2	70.6	41.3	0.80	87.2
	98041	–13	134.8	76.5	73.4	153.12 ± 0.02	22.41 ± 0.02	71.8 ± 0.3	70.8	41.6	0.92	48.0
	98117	–1	115.3	–	93.6	153.78 ± 1.25	22.40 ± 0.01	71.8 ± 0.2	70.7	41.6	0.82	24.8
	98118	–6	123.6	–	79.4	153.14 ± 0.08	22.35 ± 0.04	72.0 ± 0.3	71.0	41.7	0.83	13.0
	98119	0	110.6	–	87.6	153.17 ± 0.22	22.11 ± 0.25	71.7 ± 0.9	70.6	41.4	0.84	9.8
	98043	–4	119.8	92.7	87.6	153.21 ± 0.03	22.27 ± 0.05	71.3 ± 0.6	70.3	41.1	0.93	26.7
	98120	–2	114.5	–	94.3	152.03 ± 1.27	22.41 ± 0.15	71.7 ± 1.0	70.7	41.4	0.86	27.0
	98044	–8	126.5	79.8	77.6	153.10 ± 0.01	22.16 ± 0.02	71.5 ± 0.4	70.5	41.3	0.93	16.5
	98045	–8	116.4	96.5	92.0	153.19 ± 0.01	22.35 ± 0.01	71.7 ± 1.0	70.8	41.6	0.94	74.8
	98122	–8	123.7	–	80.9	153.10 ± 0.55	22.25 ± 0.38	72.2 ± 0.4	71.2	41.9	0.86	7.9
	98124	–4	118.8	–	94.1	152.74 ± 1.25	22.21 ± 0.01	71.5 ± 0.3	70.5	41.2	0.89	19.8
	98127	–3	113.9	–	94.3	153.39 ± 1.25	22.11 ± 0.04	70.8 ± 0.9	69.7	40.5	0.91	7.0
	98128	–2	113.2	–	95.1	153.70 ± 1.25	22.31 ± 0.02	71.2 ± 1.0	70.2	41.0	0.92	38.2
	98129	–2	116.6	–	90.0	153.32 ± 0.53	22.39 ± 0.32	70.5 ± 0.5	69.5	40.3	0.92	25.8
	98130	–4	115.9	–	92.5	153.07 ± 1.25	22.41 ± 0.02	71.6 ± 0.6	70.7	41.5	0.94	42.0
	98131	0	110.1	–	95.0	153.23 ± 1.25	22.22 ± 0.09	71.5 ± 0.4	70.5	41.3	0.94	37.6
	98132	–2	112.5	–	96.5	153.46 ± 1.32	21.99 ± 0.39	71.8 ± 0.4	70.8	41.6	0.94	28.8
	98201	–4	115.2	–	100.1	153.02 ± 0.03	22.69 ± 0.03	71.4 ± 1.7	70.3	41.1	0.27	25.3
	98202	–3	108.2	–	86.7	153.10 ± 0.08	21.88 ± 0.08	71.5 ± 0.5	70.4	41.1	0.68	9.7
	98203	–2	108.0	–	87.5	153.24 ± 0.14	21.55 ± 0.13	71.4 ± 0.9	70.3	41.0	0.76	7.8
	98204	–2	111.5	–	84.0	152.95 ± 0.09	21.36 ± 0.08	71.5 ± 0.7	70.4	41.1	0.78	10.5
	98205	–6	115.0	–	80.4	153.32 ± 0.03	22.67 ± 0.03	71.6 ± 0.1	70.6	41.4	0.80	10.2
	98082	–2	109.8	–	94.6	152.95 ± 0.05	22.40 ± 0.05	71.7 ± 0.9	70.5	41.3	0.45	29.4
	98049	0	113.7	–	107.2	153.58 ± 0.03	22.01 ± 0.03	72.5 ± 1.1	71.3	42.0	0.17	38.9
	98050	–1	120.3	106.8	103.9	153.65 ± 0.01	21.94 ± 0.01	71.9 ± 0.7	70.7	41.4	0.21	37.8
	98052	–2	118.0	96.8	95.6	153.70 ± 0.02	22.12 ± 0.01	72.0 ± 0.2	70.8	41.5	0.25	27.7
	98053	–2	118.1	101.8	90.8	153.67 ± 0.01	22.08 ± 0.01	71.8 ± 0.1	70.6	41.4	0.36	37.7
	98054	0	112.5	107.3	102.6	153.44 ± 0.01	21.60 ± 0.01	72.0 ± 1.2	70.8	41.4	0.39	41.1
	98055	0	114.8	103.2	98.5	153.72 ± 0.02	21.80 ± 0.02	71.8 ± 0.6	70.6	41.3	0.52	58.0
	98134	0	122.8	–	95.5	153.11 ± 0.03	22.41 ± 0.05	71.8± 0.4	70.6	41.3	0.34	13.6
	98059	–3	123.1	98.1	91.6	153.55 ± 0.14	21.80 ± 0.11	71.6 ± 0.4	70.5	41.2	0.66	34.3
	98135	–1	119.8	–	89.9	154.02 ± 0.10	22.03 ± 0.03	72.0 ± 0.8	70.8	41.6	0.50	18.6
	98061	0	115.2	–	96.2	153.58 ± 0.11	21.99 ± 0.10	71.8 ± 0.6	70.7	41.4	0.76	23.9
	98063	–2	120.4	–	92.2	153.81 ± 0.00	22.04 ± 0.01	71.4 ± 0.7	70.4	41.1	0.79	82.7
	98064	–5	118.9	–	80.8	153.56 ± 0.22	22.15 ± 0.20	71.8 ± 0.0	70.7	41.5	0.79	24.9
	98067	–1	114.6	–	95.1	153.68 ± 0.03	21.74 ± 0.03	71.6 ± 0.2	70.6	41.3	0.84	53.4
	98140	0	114.6	–	99.9	153.80 ± 0.19	21.90 ± 0.10	71.2 ± 0.7	70.1	40.8	0.69	45.5
	98069	–2	121.3	–	90.4	153.60 ± 0.20	21.62 ± 0.30	71.6 ± 0.7	70.6	41.3	0.85	47.4

TABLE 2. (*Continued*).

Code	mv	H_{beg}	H_{max}	H_{end}	RA_{Geo}	DEC_{Geo}	V_{inf}	V_g	V_h	COSZR	Q_{max}
98143	−2	118.0	–	92.0	153.36 ± 0.11	22.40 ± 0.10	72.3 ± 0.1	71.2	41.9	0.72	7.9
98070	−3	120.0	–	91.2	153.70 ± 0.00	21.86 ± 0.00	71.7 ± 0.2	70.6	41.4	0.87	80.3
98144	0	114.2	–	92.8	153.64 ± 0.34	22.16 ± 0.32	71.7 ± 0.2	70.6	41.3	0.74	6.7
98076	−2	117.4	–	86.8	153.74 ± 0.02	21.66 ± 0.02	71.4 ± 0.4	70.5	41.1	0.91	62.0
98147	0	117.9	–	93.2	153.76 ± 0.04	21.31 ± 0.09	71.0 ± 0.5	69.9	40.6	0.83	13.5
98148	−1	114.6	–	97.4	153.72 ± 0.04	21.67 ± 0.04	71.6 ± 0.5	70.6	41.3	0.83	62.7
98152	0	119.2	–	101.1	151.82 ± 1.88	21.57 ± 0.06	71.5 ± 0.9	70.6	41.1	0.93	36.3
98151	0	118.5	–	102.4	153.63 ± 2.93	21.36 ± 0.07	70.8 ± 0.9	69.8	40.5	0.92	34.5
98079	−1	118.2	–	95.1	154.43 ± 0.01	21.73 ± 0.00	71.7 ± 0.4	70.5	41.2	0.48	41.2
98157	0	113.1	–	101.4	154.32 ± 0.07	21.47 ± 0.02	71.8 ± 1.9	70.6	41.3	0.38	18.6
98156	−1	112.6	–	101.3	154.98 ± 1.25	21.59 ± 0.02	71.8 ± 0.4	70.6	41.4	0.40	20.3
Mean					153.29	22.12	71.6	70.5	41.3		
St. dev.					0.53	0.33	0.3	0.3	0.3		

Symbols refer to apparent meteor brightness (mv); meteor altitude at beginning of recorded trajectory (H_{beg}), peak brightness (H_{max}), and end point (H_{end}); the position of the geocentric radiant (after correction for Earth's gravity effect) given by right ascension (RA_{Geo}) and declination (DEC_{Geo}); the geocentric entry velocity (not corrected for acceleration by Earth's gravity) V_{inf}, the speed after such correction V_g; the heliocentric speed V_h; the zenith angle of entry (COSZR); and the maximum convergence angle between the planes that define the position of the trajectory (Q_{max}).

heliocentric velocity vector (radiant and speed). We consider only precise orbits with (ΔRA, ΔDEC) < 0.1° and ΔV < 1 km/s (Figs. 5 and 6). The perihelion distance (Fig. 5) and argument of perihelion (Fig. 6) are systematically smaller for the meteors photographed on 1998 November 16/17. The inclination of these meteors is also slightly smaller. Again, there is no magnitude dependence. The inclinations for 1998 November 16/17 cluster in a small region of parameter space, much as expected for a random distribution with a small dispersion. There are a few outliers. The inclinations for 1998 November 17/18 lacks such central condensation and is significantly dispersed, whereas the dispersion in perihelion distance and argument of perihelion remain similar.

The previous parameters are mostly a function of the radiant position. The speed mainly affects the semimajor axis of the orbit. The semimajor axis (*a*) is a measure of the orbital period ($P \approx a^{3/2}$), which defines whether the meteoroids are in mean motion resonances with the planets. We find that our most accurate solutions cluster in a narrow range of semimajor axis (Fig. 7). We obtain a mean value close to that of the parent comet if we accept the mean velocity of the observed trajectory as a good estimate of the preatmospheric entry velocity. If we fit an equation that weights the points later in the trajectory, where the deceleration is strongest, then we tend to find a mean value of the semimajor axis that is ~50% larger. However, the estimated uncertainties in our observations suggest such a high *a* is not genuine. For one meteor, 98003, we were able to calculate a complete single-body solution from the fish-eye picture (Spurný *et al.*, 2000). This solution supports the use of average velocities for Leonid meteors, because the exact solution gave V_{inf} = 71.207 km/s, whereas the average solution for the same record and interval of breaks gave practically the same value V_{inf} = 71.199 km/s. In conclusion, the semimajor axis of the outburst meteoroids cluster near that of the parent comet.
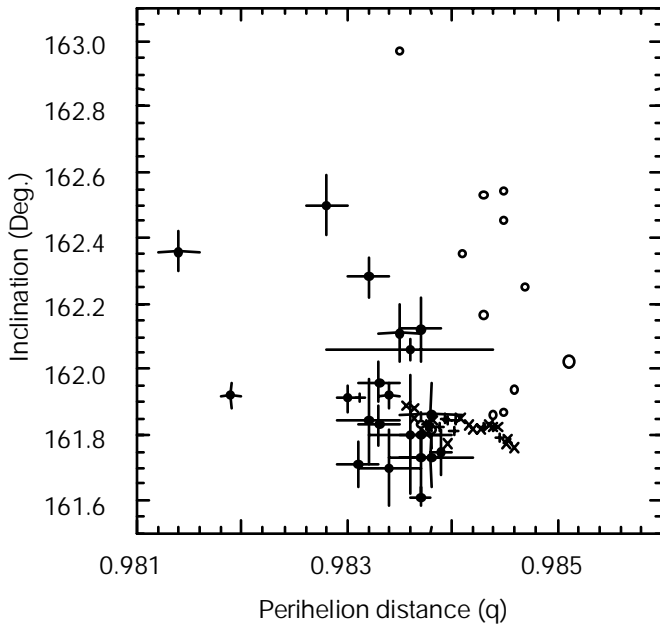
FIG. 5. Distribution of perihelion distance and inclination. Symbols as in Fig. 4. Theoretical model presented in Asher *et al.* (1999b) Fig. 1 (+) and their Fig. 2 (×).
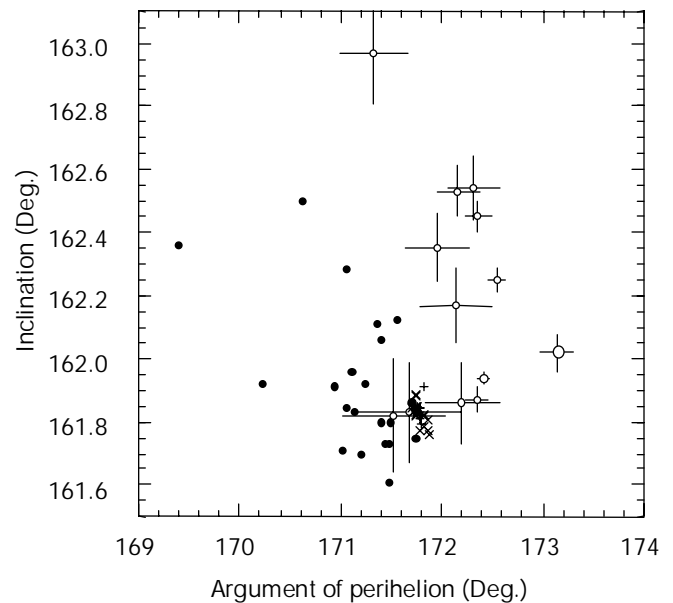
FIG. 6. Argument of perihelion as a function of inclination. Symbols as in Fig. 5.

TABLE 3. Orbital elements of 1998 Leonid meteors.

Code	Day	q	$1/a$	i	ω	node
DMS 98001	16.68186	0.9817 ± 0.0015	0.1451 ± 0.0830	161.59 ± 0.48	169.79 ± 1.18	234.12721 ± 0.00000
98002	16.69212	0.9834 ± 0.0001	0.0933 ± 0.0033	161.92 ± 0.04	171.25 ± 0.11	234.13763 ± 0.00001
98003	16.69326	0.9828 ± 0.0002	0.1539 ± 0.0017	162.50 ± 0.09	170.62 ± 0.19	234.13880 ± 0.00001
98004	16.69720	0.9833 ± 0.0002	0.1107 ± 0.0093	161.96 ± 0.06	171.11 ± 0.14	234.14266 ± 0.00000
98008	16.73461	0.9833 ± 0.0002	0.1010 ± 0.0298	161.83 ± 0.06	171.14 ± 0.19	234.18047 ± 0.00001
98011	16.75537	0.9819 ± 0.0001	0.0532 ± 0.0151	161.92 ± 0.04	170.23 ± 0.11	234.20140 ± 0.00001
98101	16.75972	0.9852 ± 0.0036	0.1086 ± 0.0473	161.97 ± 0.67	172.79 ± 3.52	234.20569 ± 0.00315
98012	16.76153	0.9831 ± 0.0002	0.0889 ± 0.0301	161.71 ± 0.07	171.02 ± 0.22	234.20761 ± 0.00001
98102	16.76676	0.9837 ± 0.0002	0.1088 ± 0.0317	161.80 ± 0.07	171.40 ± 0.21	234.21278 ± 0.00000
98013	16.76736	0.9802 ± 0.0009	0.1373 ± 0.0159	161.52 ± 0.27	168.85 ± 0.59	234.21340 ± 0.00000
98103	16.77198	0.9834 ± 0.0003	0.1094 ± 0.0578	161.70 ± 0.12	171.21 ± 0.39	234.21805 ± 0.00000
98014	16.78606	0.9833 ± 0.0008	0.0441 ± 0.1610	161.79 ± 0.33	171.25 ± 0.95	234.21825 ± 0.00000
98015	16.77279	0.9830 ± 0.0001	0.0843 ± 0.0201	161.91 ± 0.04	170.94 ± 0.13	234.21896 ± 0.00001
98105	16.77396	0.9837 ± 0.0002	0.0567 ± 0.0189	162.12 ± 0.10	171.56 ± 0.21	234.22632 ± 0.00059
98106	16.79544	0.9838 ± 0.0004	0.1195 ± 0.0195	161.73 ± 0.09	171.49 ± 0.34	234.24170 ± 0.00000
98107	16.79898	0.9821 ± 0.0004	0.1234 ± 0.0668	162.26 ± 0.17	170.18 ± 0.50	234.24525 ± 0.00000
98023	16.81479	0.9837 ± 0.0001	0.1063 ± 0.0127	161.61 ± 0.03	171.48 ± 0.09	234.26131 ± 0.00001
98109	16.81528	0.9869 ± 0.0030	0.0903 ± 0.0530	162.58 ± 0.73	174.71 ± 3.89	234.26167 ± 0.00350
98027	16.84167	0.9840 ± 0.0005	0.1033 ± 0.1139	161.85 ± 0.23	171.75 ± 0.66	234.28830 ± 0.00000
98113	16.85478	0.9832 ± 0.0002	0.0993 ± 0.0234	162.28 ± 0.06	171.06 ± 0.22	234.30151 ± 0.00000
98032	16.86150	0.9882 ± 0.0001	0.1483 ± 0.0702	162.53 ± 0.17	177.01 ± 0.27	234.30828 ± 0.00000
98031	16.86794	0.9810 ± 0.0007	0.0993 ± 0.0793	160.74 ± 0.23	169.50 ± 0.65	234.31482 ± 0.00000
98114	16.87083	0.9833 ± 0.0049	0.0991 ± 0.0226	161.53 ± 0.75	171.13 ± 3.84	234.31771 ± 0.00350
98038	16.87731	0.9836 ± 0.0008	0.1084 ± 0.0093	162.06 ± 0.03	171.41 ± 0.08	234.32423 ± 0.00000
98036	16.88233	0.9837 ± 0.0002	0.1002 ± 0.0560	161.73 ± 0.11	171.45 ± 0.33	234.32930 ± 0.00000
98040	16.88363	0.9831 ± 0.0007	0.1223 ± 0.0715	161.96 ± 0.26	170.92 ± 0.65	234.33060 ± 0.00000
98116	16.88988	0.9838 ± 0.0005	0.0985 ± 0.1159	161.92 ± 0.23	171.60 ± 0.67	234.33691 ± 0.00000
98041	16.89353	0.9839 ± 0.0001	0.0749 ± 0.0282	161.75 ± 0.07	171.73 ± 0.17	234.34069 ± 0.00001
98117	16.89722	0.9813 ± 0.0056	0.0731 ± 0.0239	161.36 ± 0.75	169.75 ± 3.75	234.34432 ± 0.00350
98118	16.90153	0.9838 ± 0.0003	0.0598 ± 0.0283	161.86 ± 0.10	171.70 ± 0.29	234.34865 ± 0.00000
98119	16.90451	0.9832 ± 0.0010	0.0929 ± 0.0843	162.15 ± 0.44	171.11 ± 0.92	234.35165 ± 0.00000
98043	16.90470	0.9832 ± 0.0003	0.1185 ± 0.0521	161.84 ± 0.13	171.07 ± 0.34	234.35195 ± 0.00001
98120	16.90556	0.9871 ± 0.0028	0.0925 ± 0.0911	162.35 ± 0.79	175.02 ± 3.94	234.35269 ± 0.00350
98044	16.90594	0.9835 ± 0.0002	0.1018 ± 0.0406	162.11 ± 0.09	171.36 ± 0.24	234.35319 ± 0.00001
98045	16.90609	0.9836 ± 0.0004	0.0738 ± 0.0940	161.80 ± 0.18	171.50 ± 0.52	234.35335 ± 0.00001
98122	16.90706	0.9839 ± 0.0021	0.0405 ± 0.0413	162.08 ± 0.69	171.79 ± 1.74	234.35422 ± 0.00000
98124	16.92569	0.9849 ± 0.0041	0.1108 ± 0.0309	162.23 ± 0.74	172.56 ± 3.89	234.37300 ± 0.00350
98127	16.93333	0.9820 ± 0.0056	0.1735 ± 0.0820	161.87 ± 0.78	169.98 ± 4.08	234.38071 ± 0.00350
98128	16.94028	0.9813 ± 0.0057	0.1299 ± 0.0950	161.44 ± 0.78	169.63 ± 3.95	234.38773 ± 0.00350
98129	16.94595	0.9828 ± 0.0023	0.1904 ± 0.0468	161.42 ± 0.61	170.54 ± 1.83	234.39344 ± 0.00000
98130	16.95417	0.9843 ± 0.0044	0.0856 ± 0.0579	161.76 ± 0.75	172.05 ± 3.82	234.40172 ± 0.00350
98131	16.95479	0.9834 ± 0.0048	0.0987 ± 0.0339	161.93 ± 0.76	171.23 ± 3.85	234.40172 ± 0.00350
98132	16.96111	0.9822 ± 0.0056	0.0751 ± 0.0392	162.22 ± 1.01	170.39 ± 4.03	234.40871 ± 0.00350
98201	17.01241	0.9850 ± 0.0006	0.1216 ± 0.1607	161.27 ± 0.32	172.58 ± 0.90	234.45046 ± 0.00000
98202	17.13900	0.9840 ± 0.0004	0.1146 ± 0.0475	162.53 ± 0.16	171.72 ± 0.39	234.58806 ± 0.00000
98203	17.17229	0.9830 ± 0.0007	0.1280 ± 0.0808	162.96 ± 0.26	170.88 ± 0.70	234.62161 ± 0.00000
98204	17.18138	0.9838 ± 0.0005	0.1223 ± 0.0689	163.46 ± 0.19	171.61 ± 0.51	234.63075 ± 0.00000
98205	17.18666	0.9847 ± 0.0001	0.0916 ± 0.0112	161.18 ± 0.06	172.43 ± 0.13	234.63615 ± 0.00000
98082	16.73877	0.9838 ± 0.0004	0.0989 ± 0.0794	161.82 ± 0.18	171.53 ± 0.51	234.18457 ± 0.00000
98049	17.67447	0.9848 ± 0.0004	0.0328 ± 0.1046	162.21 ± 0.19	172.70 ± 0.53	235.12804 ± 0.00000
98050	17.68419	0.9843 ± 0.0003	0.0925 ± 0.0618	162.17 ± 0.12	172.14 ± 0.36	235.13784 ± 0.00000
98052	17.69470	0.9845 ± 0.0001	0.0807 ± 0.0178	161.87 ± 0.04	172.35 ± 0.11	235.14846 ± 0.00000
98053	17.71869	0.9846 ± 0.0001	0.0919 ± 0.0103	161.94 ± 0.02	172.42 ± 0.06	235.17265 ± 0.00000
98054	17.72572	0.9847 ± 0.0004	0.0872 ± 0.1107	162.85 ± 0.20	172.53 ± 0.59	235.17971 ± 0.00000
98055	17.75235	0.9841 ± 0.0002	0.0986 ± 0.0542	162.35 ± 0.11	171.96 ± 0.32	235.21008 ± 0.00000
98134	17.76795	0.9867 ± 0.0001	0.0967 ± 0.0327	161.73 ± 0.10	174.71 ± 0.17	235.22234 ± 0.00000
98059	17.79340	0.9848 ± 0.0005	0.1107 ± 0.0364	162.41 ± 0.21	172.58 ± 0.52	235.24799 ± 0.00000
98135	17.80383	0.9837 ± 0.0005	0.0740 ± 0.0715	161.83 ± 0.16	171.67 ± 0.52	235.25852 ± 0.00000
98061	17.82206	0.9851 ± 0.0004	0.0905 ± 0.0534	162.13 ± 0.21	172.95 ± 0.46	235.27690 ± 0.00000
98063	17.83289	0.9844 ± 0.0002	0.1183 ± 0.0660	161.86 ± 0.13	172.20 ± 0.37	235.28784 ± 0.00000
98064	17.83319	0.9854 ± 0.0007	0.0839 ± 0.0040	161.90 ± 0.35	173.30 ± 0.73	235.28814 ± 0.00000
98067	17.85250	0.9845 ± 0.0001	0.1003 ± 0.0150	162.45 ± 0.05	172.36 ± 0.13	235.30760 ± 0.00000
98140	17.85471	0.9842 ± 0.0007	0.1444 ± 0.0600	162.05 ± 0.22	171.99 ± 0.71	235.30984 ± 0.00000
98069	17.85586	0.9846 ± 0.0008	0.1016 ± 0.0693	162.69 ± 0.51	172.47 ± 0.83	235.31254 ± 0.00000

TABLE 3. (*Continued*).

Code	Day	q	$1/a$	i	ω	node
98143	17.85938	0.9864 ± 0.0003	0.0404 ± 0.0106	161.71 ± 0.17	174.50 ± 0.35	235.31456 ± 0.00000
98070	17.86676	0.9847 ± 0.0005	0.0952 ± 0.0187	162.25 ± 0.04	172.55 ± 0.09	235.32198 ± 0.00000
98144	17.86703	0.9853 ± 0.0011	0.0973 ± 0.0221	161.82 ± 0.54	173.13 ± 1.15	235.32226 ± 0.00002
98076	17.89463	0.9843 ± 0.0002	0.1145 ± 0.0363	162.53 ± 0.08	172.16 ± 0.21	235.35008 ± 0.00000
98147	17.89942	0.9835 ± 0.0003	0.1656 ± 0.1656	162.97 ± 0.16	171.32 ± 0.33	235.35490 ± 0.00000
98148	17.89987	0.9845 ± 0.0002	0.1040 ± 0.0430	162.54 ± 0.10	172.32 ± 0.26	235.35537 ± 0.00000
98152	17.94271	0.9884 ± 0.0015	0.1170 ± 0.0842	163.80 ± 1.09	178.25 ± 5.99	235.38530 ± 0.00525
98151	17.94271	0.9842 ± 0.0068	0.1774 ± 0.0861	162.95 ± 1.15	171.92 ± 6.18	235.39856 ± 0.00525
98079	18.74645	0.9851 ± 0.0001	0.1099 ± 0.0326	162.02 ± 0.06	173.14 ± 0.17	236.20943 ± 0.00000
98157	18.78128	0.9853 ± 0.0005	0.1010 ± 0.1738	162.52 ± 0.33	173.33 ± 0.88	236.24457 ± 0.00000
98156	18.78128	0.9833 ± 0.0047	0.0956 ± 0.0368	161.93 ± 0.75	171.46 ± 3.87	236.24459 ± 0.00350
Mean		0.9839	0.1027	162.05	171.89	
St.Dev.		0.0014	0.0299	0.49	1.50	

Symbols are: perihelion distance (q, in AU), semimajor axis (a, in AU), inclination (i, degrees), argument of perihelion (ω, degrees), and ascending node (node, degrees).
*Orbits 98201,202,203,204, and 205 are computed from data of the meteor section of the British Astronomical Association.

TABLE 4. Data as in Tables 2 and 3 for Leonid orbits with unusually short semimajor axis (low entry velocity).

Code	mv	H_{beg}	H_{max}	H_{end}	RA_{Geo}	DEC_{Geo}	V_{inf}	V_g	V_h	COSZR	Q_{max}
98006	−1	99.2	87.5	78.2	152.19 ± 0.02	22.02 ± 0.01	62.2 ± 0.4	60.8	31.6	0.48	35.6
98108	0	119.9	–	103.8	154.66 ± 1.87	21.18 ± 1.31	70.2 ± 0.4	68.9	39.6	0.44	3.9
98020	−4	122.8	95.7	88.5	153.21 ± 0.01	21.82 ± 0.02	70.4 ± 0.3	69.2	40.0	0.70	28.3

Code	Day	q	$1/a$	i	ω	node
98006	16.7333	0.9722 ± 0.0036	0.897 ± 0.029	160.65 ± 0.12	148.41 ± 6.34	234.1791 ± 0.0000
98108	16.8014	0.9667 ± 0.0163	0.254 ± 0.041	164.02 ± 2.44	161.40 ± 6.77	234.2476 ± 0.0035
98020	16.8054	0.9813 ± 0.0002	0.221 ± 0.028	162.34 ± 0.06	169.28 ± 0.25	234.2518 ± 0.0000

Three orbits are outliers. Each has a semimajor axis significantly less than the mean of all orbits. All three were detected on 1998 November 16/17. They have a significantly larger dispersion in radiant position. Although the radiant identifies each meteor as a Leonid, the measured speed is much less than that of the mean. This type of orbit can only occur after a close encounter with Earth, and we conclude that 3 out of 98 Leonid meteoroids had a previous encounter with Earth. In order to detect a significant number of such meteoroids, Earth would have had to cross the stream numerous times before.

DISCUSSION

At least three dust components were identified in the meteor rate curve during the 1998 November return (Arlt, 1998; Betlem and van Mil, 1999; Jenniskens, 1999). A one-day wide component rich in bright fireballs was responsible for most, if not all, of the Leonid meteors detected on 1998 November 16/17. On top of that, a narrow peak was observed to span the period between 16 and 21.5 UT on 1998 November 17/18.

These dust components are also manifested in the measured orbital elements. The systematic displacements of the 1998 November 16/17 and 17/18 distributions of perihelion distance and inclination suggest an origin at different epochs or a different orbital evolution since ejection.

The broad 1998 November 16/17 component rich in bright meteors was recently ascribed to matter trapped in orbital resonances, specifically ejecta from the return of 1333 (Asher *et al.*, 1999a). The model orbital parameters were kindly provided

byAsher (pers. comm.) and are from data presented in Fig. 1 (+) and Fig. 2 (×) of the follow-up paper by Asher *et al.* (1999b). The theoretical data are shown as crosses in Figs. 5 and 6. We selected only those orbits that pass within 0.0005 AU from Earth's orbit (other orbits mainly extend the observed range to higher I and q, without changing ω).

We find that the mean inclination matches well with the observations. The perihelion distance and argument of perihelion are slightly less than the theoretical value. This result appears to
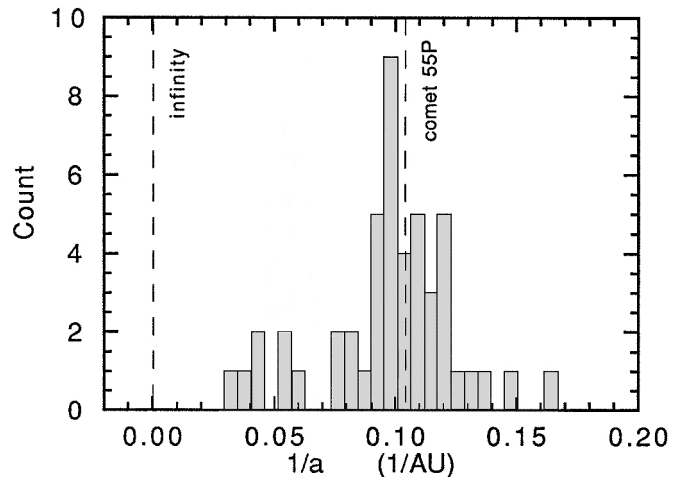
FIG. 7. Histogram of semimajor axis of meteoroid orbits, in terms of $1/a$.

confirm that the broad component of large grains is in orbital resonance as proposed by Asher *et al.* The observed relatively narrow range in semimajor axis is consistent with such trapping.

One inconsistency is the relatively large dispersion of measured orbital elements. The Asher *et al.* model of ejection in 1333 suggests a very narrow distribution of orbital elements. Especially the argument of perihelion and inclination are in a narrow range, much narrower than observed. The trapped debris must be a compilation from more than a single return, with similar orbital period but slightly different I, q, and ω (Jenniskens and Betlem, 1999).

In the Asher *et al.* model, other dust components are not in resonant orbits. Indeed, the larger dispersion in inclination on 1998 November 17/18 is consistent with this matter being in nonresonant orbits. However, recent models typically ascribe narrow components to ejecta that are only 2–4 revolutions old (*e.g.*, Kondrat'eva and Reznikov, 1985; Asher, 1999; Asher *et al.*, 1999a). Such models can not account for the observed dispersion. If the radiant dispersion is due to ejection velocities only, then the typical ejection velocity should be ~100 m/s, which is much larger than typically assumed—on the order of 1–10 m/s for the relevant mass range (Jenniskens, 1998). It is possible that the observed narrow peak is due to relatively old ejecta, because Earth did not pass close to debris trails ejected in recent returns. In that case, the peak may be a composite of ejecta from different epochs as proposed by Jenniskens (1999), and the dispersion in inclination may reflect planetary perturbations of the comet orbit from one return to the next.

Further modeling is warranted, because the present orbits (Asher *et al.*, 1999b) only cover a few hours around the peak of the shower and represent only the central part of the observed fireball outburst.

REFERENCES

ARLT R. (1998) Bulletin 13 of the International Leonid Watch: The 1998 Leonid Meteor Shower. *WGN, the Journal of the IMO* **26,** 239–248.

ASHER D. J. (1999) The Leonid meteor storms of 1833 and 1966. *Mon. Not. R. Astron. Soc.* **307,** 919–924.

ASHER D. J., BAILEY M. E. AND EMEL'YANENKO V. V. (1999a) Resonant meteoroids from Comet Tempel–Tuttle in 1333: The cause of the unexpected Leonid outburst in 1998. *Mon. Not. R. Astron. Soc.* **304,** L53–L56.

ASHER D. J., BAILEY M. E. AND EMEL'YANENKO V. V. (1999b) The resonant Leonid trail from 1833. *Irish Astr. J.* **26,** 91–93.

BETLEM H. AND VAN MIL O. (1999) Leoniden 1998. Visuele Resultaten. *Radiant, J. Dutch Met. Soc.* **21,** 65–72.

BETLEM H., TER KUILE C. R., VAN 'T LEVEN J., DE LIGNIE M., RAMON BELLOT L., KOOP M., ANGELOS C., WILSON M. AND JENNISKENS P. (1997) Precisely reduced meteoroid trajectories and orbits from the 1995 Leonid meteor outburst. *Planet. Space Sci.* **45,** 853–856.

BETLEM H., TER KUILE C. R., DE LIGNIE M., VAN 'T LEVEN J., JOBSE K., MISKOTTE K. AND JENNISKENS P. (1998) Precision meteor orbits obtained by the Dutch Meteor Society—Photographic Meteor Survey (1981–1993). *Astron. Astrophys. Suppl. Ser.* **128,** 179–185.

CEPLECHA Z., BOROVICKA J., ELFORD W. G., REVELLE D. O., HAWKES R. L., PORUBCAN V. AND SIMEK M. (1998) Meteor phenomena and bodies. *Space Sci. Rev.* **84,** 327–471.

JENNISKENS P. (1996) Meteor stream activity III. Measurement of the first in a new series of Leonid outburst. *Meteorit. Planet. Sci.* **31,** 177–184.

JENNISKENS P. (1998) On the dynamics of meteoroid streams. *Earth Planets Space* **50,** 555–567.

JENNISKENS P. (1999) Activity of the 1998 Leonid shower from video records. *Meteorit. Planet. Sci.* **34,** 959–968

JENNISKENS P. AND BETLEM H. (2000) Massive remnant of evolved cometary dust trail detected in the orbit of Halley-type comet 55P/Tempel–Tuttle. *Astrophys. J.* (in press).

JENNISKENS P. AND BUTOW S. J. (1999) The 1998 multi-instrument aircraft campaign—an early review. *Meteorit. Planet. Sci.* **34,** 933–943.

KONDRAT'EVA E. D. AND REZNIKOV E. A. (1985) Comet Tempel–Tuttle and the Leonid meteor swarm. *Sol. Syst. Res.* **31,** 489–492.

LANGBROEK M. (1999) Leonid outburst activity 1996: A broad structure and a first occurrence of a narrow peak of fainter meteors. *Meteorit. Planet. Sci.* **34,** 137–145.

SPURNÝ P., BETLEM H., VAN 'T LEVEN J. AND JENNISKENS P (2000) Atmospheric behavior and extreme beginning heights of the 13 brightest photographic Leonids from the ground-based expedition to China. *Meteorit. Planet. Sci.* **35,** (in press).